THE JOURNAL OF BIOLOGICAL CHEMISTRY VOL. 291, NO. 8, pp. 3785–3795, February 19, 2016

Wilms Tumor Suppressor, WT1, Cooperates with MicroRNA-26a and MicroRNA-101 to Suppress Translation of the Polycomb Protein, EZH2, in Mesenchymal Stem Cells*

Received for publication, July 24, 2015, and in revised form, December 9, 2015 Published, JBC Papers in Press, December 10, 2015, DOI 10.1074/jbc.M115.678029

Murielle M. Akpa[‡], Diana Iglesias[§], LeeLee Chu[§], Antonin Thiébaut[§], Ida Jentoft[§], Leah Hammond[§], Elena Torban[¶], and Paul R. Goodyer[‡§¶1]

From the [‡]Department of Human Genetics, McGill University, Montréal, Québec H3A 1B1, the [¶]Department of Experimental Medicine, McGill University, Montreal, Québec H3A 1A3, and the [§]Department of Pediatrics, Research Institute of the McGill University Health Center, Montréal, Québec H4A 3J1, Canada

Hereditary forms of Wilms arise from developmentally arrested clones of renal progenitor cells with biallelic mutations of *WT1*; recently, it has been found that Wilms tumors may also be associated with biallelic mutations in *DICER1* or *DROSHA*, crucial for miRNA biogenesis. We have previously shown that a critical role for WT1 during normal nephrogenesis is to suppress transcription of the Polycomb group protein, *EZH2*, thereby de-repressing genes in the differentiation cascade. Here we show that WT1 also suppresses translation of *EZH2*. All major WT1 isoforms induce an array of miRNAs, which target the 3′ UTR of *EZH2* and other Polycomb-associated transcripts. We show that the WT1(+KTS) isoform binds to the 5′ UTR of *EZH2* and interacts directly with the miRNA-containing RISC to enhance post-transcriptional inhibition. These observations suggest a novel mechanism through which WT1 regulates the transition from resting stem cell to activated progenitor cell during nephrogenesis. Our findings also offer a plausible explanation for the fact that Wilms tumors can arise either from loss of WT1 or loss of miRNA processing enzymes.

In 1879, William Osler reported two pediatric patients from Montreal with massive kidney tumors containing bands of muscle-like tissue mixed with epithelial elements (35). Twenty years later, Max Wilms published his celebrated monograph recognizing the malignancy as a unique "mischgeschwulste der Niere" (mixed tumor of the kidney), composed of mixed stromal, epithelial, and undifferentiated mesenchymal cells. This "triphasic" histology suggests that Wilms tumors arise from developmentally arrested stem cells of the metanephric mesenchyme that occasionally exhibit abortive differentiation toward a stromal or an epithelial cell fate. It follows that a disturbance of molecular events governing the transition from renal progenitor cells into these differentiated lineages must be central to the pathogenesis of Wilms tumor.

Wilms tumor (WT)[2] is the most common form of pediatric kidney cancer and affects about 1:10,000 children in North America (1). In a subset of these patients, a germline deletion of the transcription factor, WT1, is accompanied by a somatic mutation of the second *WT1* allele, giving rise to clones of incompetent stem cells adjacent to the malignant tumor (2). These "nephrogenic rests" are thought to represent embryonic renal progenitors that have failed to respond to inductive WNT signals during embryogenesis. The pre-malignant cell clusters may persist within the normal kidney (3) until a constitutively activating mutation of the β-catenin gene (*CTNNB1*) (17, 18) bypasses the need for a normal WNT signal and drives un-regulated rapid cell growth (4). Wilms tumors retain a chromatin pattern resembling embryonic stem cells in which genes of the differentiation cascade are broadly silenced by tri-methylated lysine 27 residues in the H3 histone associated with their promoter regions (5). We recently showed that the WT1 isoforms lacking the three amino acid insertion lysine-threonine-serine between zinc fingers 3 and 4 (−KTS), inhibits transcription of the histone methyltransferase (Enhancer of Zeste Homolog 2, *EZH2*) that epigenetically silences β-catenin gene (*CTNNB1*) expression in mesenchymal stem cells and facilitates the canonical WNT/β-catenin pathway response to WNT9b (6).

Only about 20% of Wilms tumors are linked to *WT1* mutations (7, 8). Recently, it was discovered that a subset of Wilms tumors with normal *WT1* alleles are associated with mutations of either *DICER1* (9) or *DROSHA* (10). These genes encode proteins that process microRNAs (miRNAs), implying that loss of either WT1 or miRNA biogenesis can lead to the same Wilms tumor phenotype. We reasoned that the crucial effects of WT1 during development might require both transcriptional and miRNA-mediated post-transcriptional inhibition of EZH2. Here we show that WT1 is evident both in the nucleus and cytoplasm of progenitor cells in embryonic mouse kidney nephrogenic mesenchyme. In mesenchymal stem cells isolated from human amniotic fluid, we show that WT1 induces expression of multiple miRNAs, including miRNA-26a (miR-26a) and miRNA-101 (miR-101). In fibroblasts, we show that the latter

* This work was supported in part by Operating Grant MOP-119571 from the Canadian Institutes of Health Research (CIHR) and an infrastructure support grant to the McGill University Health Center Research Institute from the Fonds de la Recherche en Santé du Québec (FRSQ). The authors declare that they have no conflicts of interest with the contents of this article.

[1] Recipient of a James McGill Research Chair. To whom correspondence should be addressed: Depts. of Human Genetics and Pediatrics, Montreal Children's Hospital Research Institute, 1001 Décarie Blvd., Bloc E, Lab E012371, Montreal, QC H4A 3J1, Canada. Tel.: 514-412-4400 (ext. 22584); Fax: 514-412-4478; E-mail: paul.goodyer@mcgill.ca.

[2] The abbreviations used are: WT, Wilms tumor; KTS, lysine-threonine-serine; miRNA, microRNA; mir-26a, microRNA-26a; miR-101, microRNA-101; RISC, RNA-induced silencing complex; amMSC, amniotic fluid-derived mesenchymal stem cell; EZH2, Enhancer of Zeste Homolog 2; qPCR, quantitative PCR.

two miRNAs suppress *EZH2* translation. Furthermore, we show that WT1 binds to the 5′ untranslated region (UTR) of *EZH2* mRNA and cooperates with miRNA-containing RNA-induced silencing complexes (RISCs) to suppress EZH2 translation. These observations suggest a novel mechanism through which the WT1 transcription factor exerts post-transcriptional regulation in cooperation with miRNAs.

Experimental Procedures

Cell Culture—Human amniotic fluid-derived mesenchymal stem cells (amMSC) were grown in the presence of DMEM culture medium (Gibco, Life Technologies, Burlington, ON, Canada) with 15% fetal bovine serum (Wisent, Saint-Jean-Baptiste, QC, Canada) and 1% penicillin/streptomycin (Gibco). Human fibroblasts (MCH070) and mouse mesonephric kidney cells (M15) (11) were grown in DMEM culture medium (Gibco) with 10% fetal bovine serum (Wisent) and 1% penicillin/streptomycin (Gibco).

Viral Particle Transduction—amMSC were transduced with viral particles expressing the two principal subgroups of human WT1 isoforms containing exon 5 (17 amino acid sequence) with (+/+) or without (+/−) the KTS insertion in exon 9 or control GFP particles. The WT1 isoforms cDNA were cloned into the pWPI bicistronic vector (Dr. Trono Lab/Addgene). Each plasmid was co-transfected with pMD2.G, the envelope plasmid, and psPAX2, the packaging plasmid, into 293T cells. Viral particles were harvested and used for the transduction. Specific WT1 isoforms are denoted by plus or minus symbols; the first indicating the presence or absence of a 17-amino acid sequence in exon 5 and the second KTS between zinc fingers 3 and 4 status.

Immunoprecipitation—Cells were grown and harvested following standard techniques. Cell lysis buffer contained Tris (10 mM, pH 7.4), NaCl (10 mM), $MgCl_2$ (3 mM), Nonidet P-40 (0.3%), and glycerol (10%). The immunoprecipitation was performed using Protein A/G-agarose beads. The following antibodies and titers were used: normal rabbit IgG (2729, 2 μg, Cell Signaling, Danvers, MA), WT1 C19 (sc192, 2 μg, Santa Cruz Biotechnology, Inc., Santa Cruz, CA), anti-Ago2/eIF2C2 (ab32381, 2 μg, Abcam, Toronto, ON, Canada), and anti-Dicer (ab14601, 2 μg, Abcam).

Immunoblotting—Following the immunoprecipitations, 6× loading dye was added to the Protein A/G-agarose beads, boiled at 95 °C for 8 min, loaded onto SDS-PAGE gel, and subjected to electrophoresis following standard immunoblotting techniques. The following primary antibodies and titers were used: WT1 C19 (sc192, 1/200, Santa Cruz Biotechnology, Inc.), anti-Ago2/eIF2C2 (ab32381, 1/500, Abcam), and anti-Dicer (ab4735, 1/500, Abcam). Immunoreactive bands were detected using species-specific horseradish peroxidase-conjugated secondary antibodies (1/2000, Cell Signaling) and visualized using GE Healthcare ECL Plus Western blotting Detection Reagents and the Storm Imager Scanner and software (GE Healthcare, Mississauga, ON, Canada).

Indirect Immunofluorescence Staining—Cryosections (5 μm) from embryonic mouse kidneys at 17.5 dpc stage were fixed with acetone at −20 °C for 7 min, incubated in 1% Triton X-100, PBS for 30 min, blocked with normal goat serum (10% in 1% BSA, 0.1% Triton X-100/PBS) for 1 h, and incubated with primary antibody WT1 C19 (sc192, 1/400, Santa Cruz Biotechnology, Inc.) and Alexa Fluor® 568-conjugated secondary antibodies (1/1000) at 4 °C overnight and room temperature for 1 h, respectively. The sections were also incubated with *Dolichos biflorus* agglutinin antibody (1/300, Vector Laboratories, Inc., Burlingame, CA) and the nuclei were counterstained with DAPI. Images were obtained with a laser scanning confocal microscope (LSM780) and the ZEN2010 software (Carl Zeiss Canada Ltd., Toronto, ON, Canada) at room temperature and processed by Adobe Photoshop and Illustrator software.

RNA Isolation and Real-time PCR Analysis—RNA, including miRNA, was purified using the miRNeasy mini kit according to the manufacturer's instructions (Qiagen, Toronto, ON, Canada). Reverse transcription for mRNA was done with the iScript cDNA synthesis kit (Bio-Rad), and for miRNA using the miScript II RT kit (Qiagen, Toronto, ON, Canada). Quantitative PCR for reverse transcribed mRNA was performed using with the SsoFast EvaGreen Supermix with Low ROX (Bio-Rad) and specific primer sets. Quantitative PCR for reverse transcribed miRNA was performed using the miScript SYBR Green PCR kit and specific primer assays for miRNA (Qiagen). Both PCR were performed in a LightCycler 480 II (Roche Applied Science, Laval, QC, Canada).

miRNA Expression Profile—RNA was extracted and sent for miRNA microarray and analysis (EXIQON, Vedbæk, Denmark). The samples were labeled using the miRCURY LNA™ microRNA Hi-Power Labeling Kit, Hy3™/Hy5™, and hybridized on the miRCURY LNA™ microRNA array (7th generation), following a dual color experimental design.

Transfection—Human fibroblasts (MCH070 cells) were transfected with pCMVSport6, pCMVSport6/hEZH2FL (insert size about 1.1 kb) (ATCC, MGC Human Clones, image ID: 3901250), WT1 cloned into a pcDNA3.1/Zeo(+) vector (kindly provided by Dr. P. Grundy, Calgary, AB, Canada), miScript miRNA mimics: Syn-hsa-miR-26a-5p, Syn-hsa-miR-101–3p, Syn-hsa-miR-93, and AllStars Negative Control siRNA, miScript miRNA inhibitor: anti-hsa-miR-26a-5p, anti-hsa-miR-101–3p, anti-hsa-miR-93, and miScript Inhibitor Negative Control (Qiagen) using Lipofectamine® 2000 transfection reagent according to the manufacturer's instructions (Invitrogen).

Electromobility Shift Assay—Synthetic oligonucleotides to the 5′ UTR of *EZH2* were labeled by back filling with the Klenow fragment of DNA polymerase I using [α-^{32}P]dCTP (3000 Ci/mmol) (PerkinElmer Life Science). WT1 protein was synthesized using a T7-coupled transcription/translation reticulocyte lysate system. The *in vitro* translated products were incubated with ^{32}P-labeled probes at room temperature for 15 min in a solution containing 4% Ficoll, 1 mM EDTA (pH 8.0), 10 mM HEPES (pH 7.9), 1 mM dithiothreitol (DTT), and 1 μg of poly(dI)·poly(dC). For specificity tests, the protein preparation was preincubated with 1 μg of anti-WT1 (C-19) antibody for 20 min at room temperature and then incubated with the radiolabeled probe for 20 min at room temperature. For competition experiments, reaction mixtures were preincubated for 15 min at room temperature with unlabeled oligonucleotide prior to the addition of radiolabeled probes. Following the binding step,

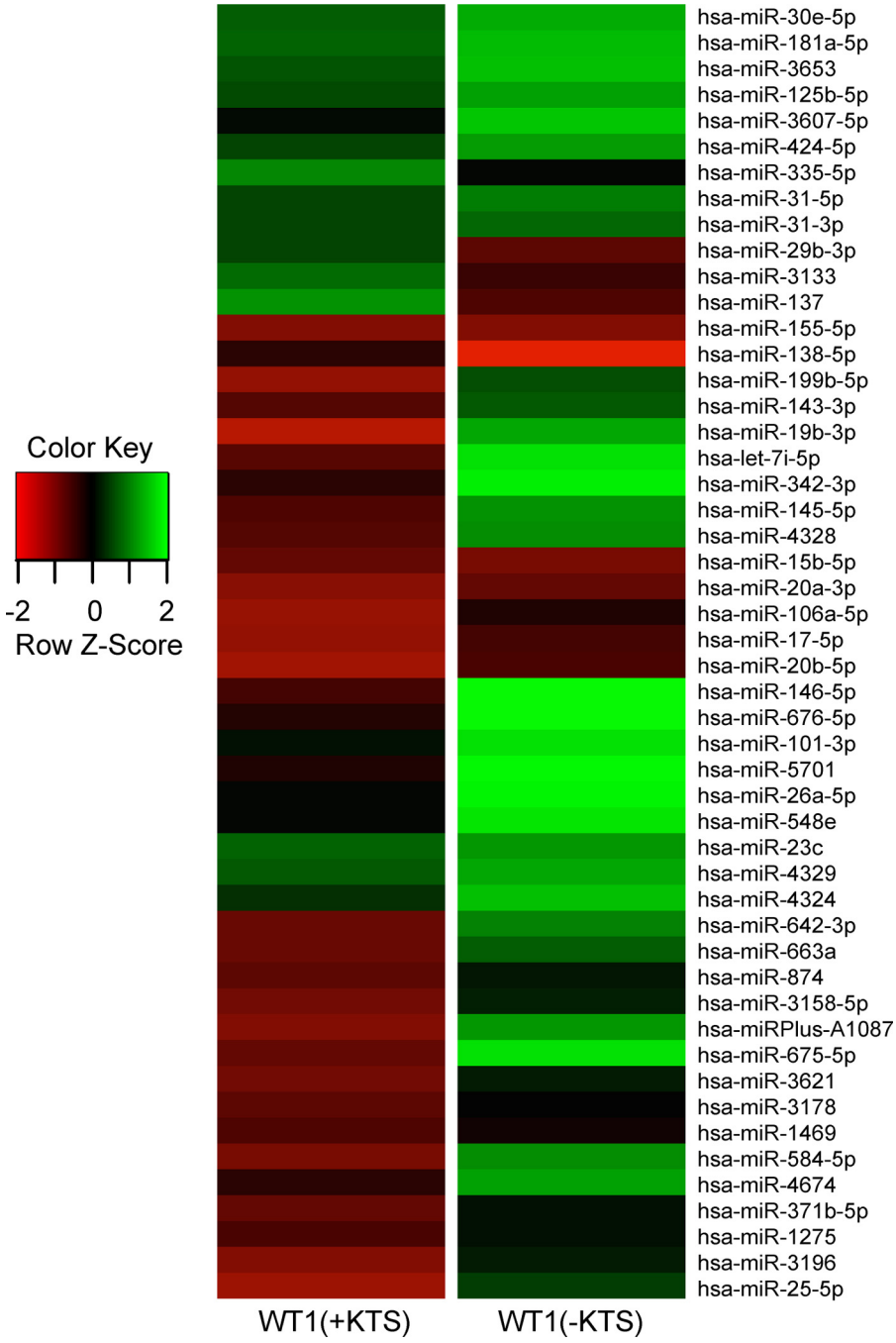

FIGURE 1. **miRNA expression profile.** The heat map shows the differential expression pattern of miRNAs in mesenchymal stem cells stably transfected with WT1 (+KTS) or WT1(−KTS) isoforms relative to the overall mean for both cell lines and an empty vector control. Each row represents a microRNA and its expression level relative to control. *Red* represents expression below the mean; *green* represents expression above the mean.

reaction mixtures were electrophoresed on a 6% polyacrylamide gel (acrylamide/bis-acrylamide ratio, 29:1) in 0.25× TBE buffer (22.25 mM Tris·HCl, 22.25 mM boric acid, and 1 mM EDTA) at 90 V at room temperature. The gels were dried and exposed to Kodak X-Omat film at room temperature.

RNA Immunoprecipitation Assay-qPCR—Cells were grown and harvested using 0.25% trypsin/EDTA (Gibco) following standard techniques and resuspended in RIP buffer (150 mM KCl, 25 mM Tris, pH 7.4, 5 mM EDTA, 0.5 mM DTT, 0.5% Nonidet P-40, 100 units/ml of RNase inhibitor and protease inhibitor). Embryonic mouse kidney at 17 dpc stage were flash frozen and pulverized using standard protocol and resuspended in RIP buffer. Sonication was performed on a Sonolab 7.1 (Covaris, Toronto, ON, Canada). The immunoprecipitation was performed using Protein A/G-agarose beads. The following antibodies and titers were used: normal rabbit IgG (2729, 2 μg, Cell Signaling), WT1 C19 (sc192, 2 μg, Santa Cruz Biotechnology, Inc.), and anti-Ago2/eIF2C2 (ab32381, 2 μg, Abcam). Purification of the RNA bound to the RNA-binding proteins was performed using the miRNeasy mini kit according to the manufacturer's instructions (Qiagen). cDNA synthesis was performed as mentioned before. Primers for the qPCR are miScript Primer

TABLE 1

Up-regulated miRNAs targeting Polycomb group and associated proteins

16 of 32 WT1-induced miRNAs have putative seed sequences in the 3′ UTR of *EZH2* and various Polycomb-associated proteins.

	EZH2	*EED*	*SUZ12*	*DNMT3A*	*DNMT3B*	*DNMT1*	*JARID*
hsa-let-7i-5p	X						
hsa-miR-101–3p	X	X	X	X	X		X
hsa-miR-125b-5p	X	X	X	X	X	X	X
hsa-miR106a-5p	X	X	X	X	X	X	X
hsa-miR-146b-5p	X	X	X	X	X	X	X
hsa-miR-17–5p	X	X	X	X	X	X	X
hsa-miR-181a-5p	X	X	X	X	X	X	X
hsa-miR-19c-3p	X	X	X	X	X	X	X
hsa-miR-25–5p	X	X	X	X	X	X	X
hsa-miR-26a-5p	X						
hsa-miR-29b-3p	X	X	X	X	X	X	X
hsa-miR-31–5p	X	X	X	X	X	X	X
hsa-miR-335–5p					X		
hsa-miR-4328				X		X	
hsa-miR-4674				X	X		
hsa-miR-584–5p				X		X	

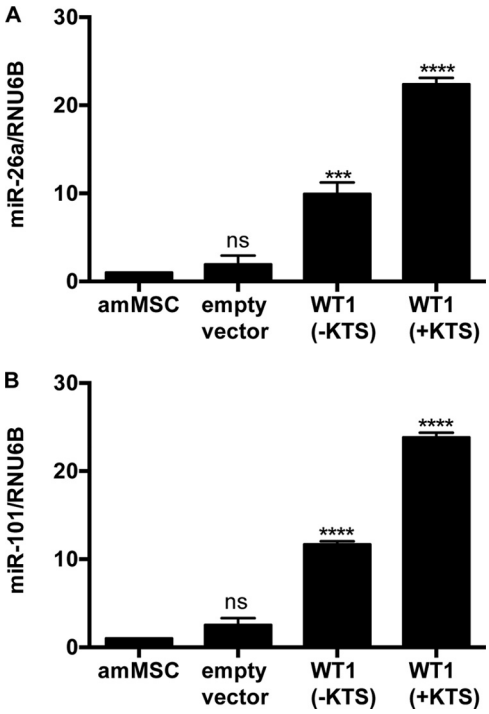

FIGURE 2. **Validation of selected miRNAs.** *A*, miR-26a levels were quantified ($n = 3$) by qRT-PCR with *RNU6B* as the reference miRNA transcript in various cell lines. *B*, miR-101 levels were quantified ($n = 3$), using *RNU6B* for normalization. One-way analysis of variance with Dunnett's multiple comparison tests *versus* parental amMSC line: $p < 0.0001$ (****), $p < 0.001$ (***), not significant (*ns*).

Assays Hs_miR-26a_1, Hs_miR-101_3, and Hs_ miR-93 (Qiagen), as well as qPCR primers designed for the detection of the *EZH2* gene (EZH2 forward: 5′-TTGTTGGCGGAAGCGTGTAAAATC and EZH2 reverse: 5′-TCCCTAGTCCCGCGCAATGAGC.

Statistical Analysis—Data are presented as mean ± S.E. of three or more independent results. Statistical significance was assessed using *t* test, one-way or two-way analysis of variance followed by comparison tests.

Results

WT1 Induces an Array of miRNAs in Mesenchymal Stem Cells—Because mutations of *WT1* or *DICER1* lead to a similar Wilms tumor phenotype, we reasoned that WT1 might normally induce key miRNAs in metanephric mesenchyme that are essential for differentiation. We isolated RNA from human mesenchymal stem cells (6) stably transduced with either a WT1(−KTS) or a WT1(+KTS) isoform. Fig. 1 shows the miRNA heat map, indicating up-regulation (>2-fold) of 12 miRNAs in the WT1(+KTS)-expressing cell line and 28 miRNAs in the WT1(−KTS) cell line, compared with the mean for parental and empty vector-transfected controls. Eight of the WT1(+KTS) miRNAs overlapped with the WT1(−KTS) group, giving a total of 32 miRNAs induced by one isoform or the other. Because our previous studies suggest that down-regulation of EZH2 is a crucial event in de-repressing genes of the differentiation cascade (6), we screened the 3′ UTR of EZH2 for seed sequences for these 32 miRNAs. Interestingly, 16/32 miRNAs are predicted to target members of the Polycomb complex or associated methyltransferases, of these, 12/16 are predicted to target the *EZH2* 3′ UTR (Table 1). These 12 included miR26a and miR101, previously shown to suppress translation of EZH2 in myocytes, lung tissue, and breast epithelia, respectively (12–15). We decided to focus on these latter

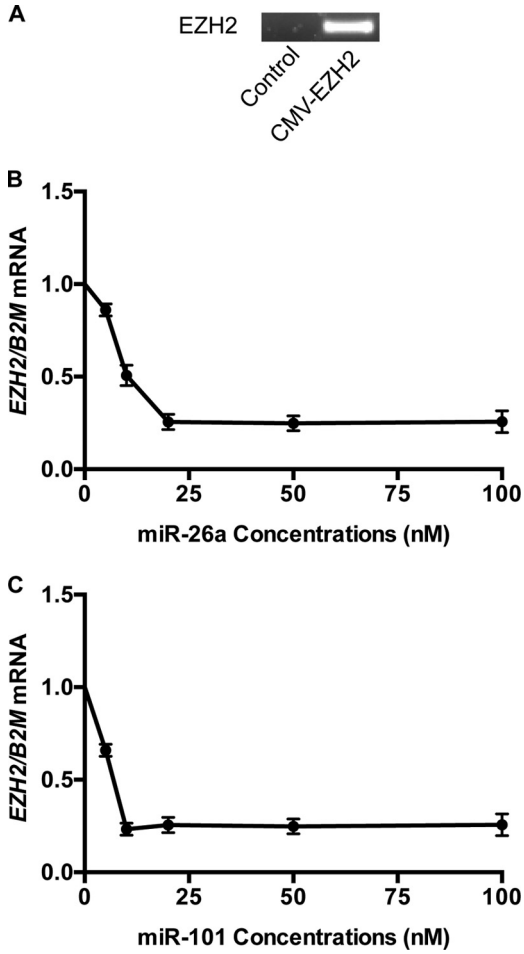

FIGURE 3. **Effect of different miRNA concentrations on exogenous EZH2.** *A*, absence of endogenous EZH2 transcript in control human fibroblasts *versus* fibroblasts transfected with CMV-EZH2 expression plasmid. *B*, dose-response curve showing the effect of various concentrations of miR-26a on the expression of exogenous *EZH2* mRNA. The minimal dose with the maximum effect is 25 nM ($n = 4$). *C*, dose-response curve showing the effect of various concentrations of miR-101 on the expression of exogenous EZH2. The minimal dose with the maximum effect is 20 nM ($n = 4$).

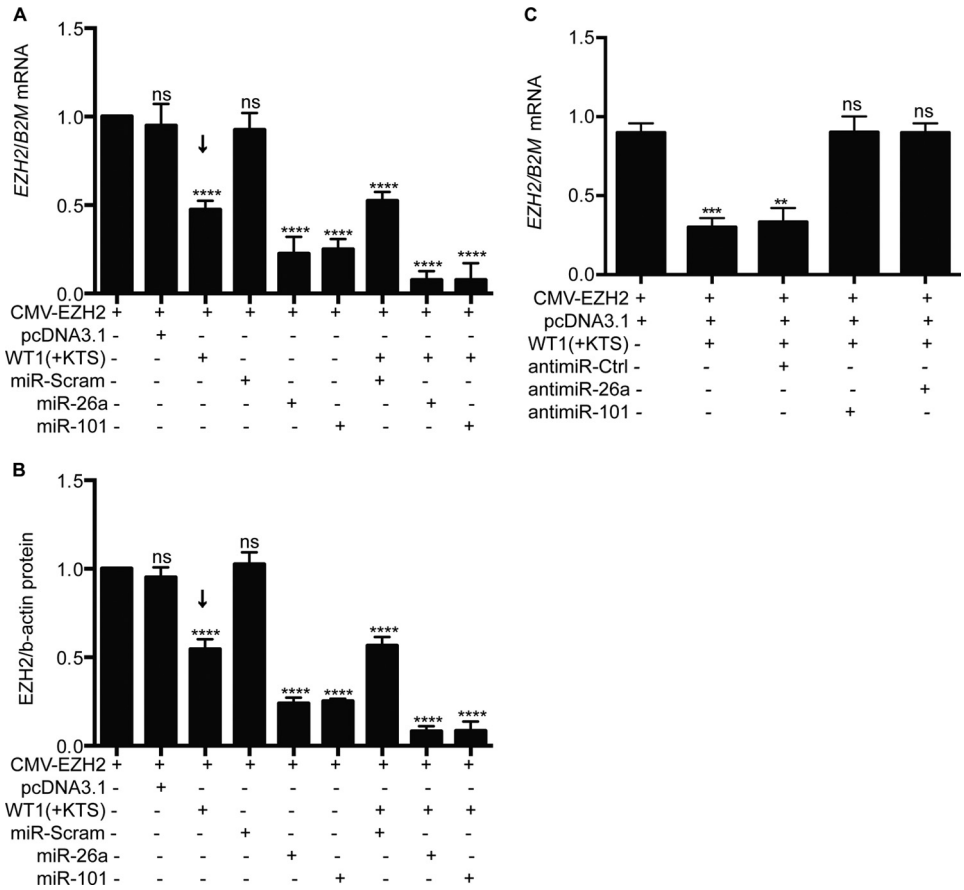

FIGURE 4. **WT1 cooperates with miRNAs to inhibit EZH2 expression.** *A,* levels of *EZH2* mRNA were quantified by qRT-PCR ($n = 4$) and normalized to β_2-microglobulin (*B2M*) in human fibroblasts transiently transfected with EZH2, WT1, miR-26a, miR-101, or their control plasmids. *B,* levels of EZH2 protein were quantified by densitometric analysis of Western immunoblots normalized for β-actin ($n = 4$) in human fibroblasts transiently transfected as above. *C,* levels of *EZH2* mRNA were quantified by qRT-PCR ($n = 4$) and normalized to *B2M* in human fibroblasts transiently transfected with EZH2, WT1, anti-miR-26a, anti-miR-101, or their control plasmids. One-way analysis of variance with Dunnett's multiple comparison tests for each experimental cell line *versus* baseline cells transfected with EZH2 only: $p < 0.0001$ (****), $p < 0.001$ (***), not significant (*ns*).

two miRNAs as representative of the putative concerted mechanism by which WT1 suppresses epigenetic silencing in stem cells (6). To validate these two miRNAs, we performed quantitative RT-PCR on mesenchymal stem cells stably transfected with WT1(−KTS) or WT1(+KTS) isoforms. As seen in Fig. 2, miR-26a and miR-101 levels were significantly increased in both cell lines expressing WT1.

miR-26a and miR-101 Cooperate with WT1 to Suppress EZH2 Translation—To confirm that miR-26a and miR-101 suppress *EZH2* translation, we transfected human fibroblasts with an expression plasmid containing the full-length *EZH2* mRNA driven by a CMV promoter; at baseline, fibroblasts had no detectable endogenous EZH2 or WT1. In the transfected cells, we confirmed high levels of exogenous EZH2 transcript (Fig. 3*A*). When fibroblasts were transfected with varying amounts of miR-26a or miR-101 mimics, we noted maximal suppression of EZH2 with 25 nM miR-26a vector and 20 nM miR-101 (Fig. 3*B*). In previous studies, we noted that the WT1(+KTS) isoforms suppress EZH2 protein levels in mesenchymal stem cells (6). If this effect is due to transcriptional inhibition, there should be no effect of WT1(+KTS) on the CMV-driven EZH2 expression in fibroblasts. However, when we transiently transfected fibroblasts with WT1(+KTS), we noted a 50% reduction (*arrows*) in exogenous EZH2 mRNA and protein levels (Fig. 4, *A* and *B*). When WT1(+KTS) was combined with miR-26a or miR-101 mimics (25 nM), EZH2 expression was further suppressed to 10–15% of baseline (Fig. 4, *A* and *B*).

To confirm that the effect of WT1(+KTS) on the exogenous *EZH2* transcript is mediated by endogenous miRNAs, we preformed rescue experiments with antago-miRs specific for miR-101 and miR-26a. As seen in Fig. 4*C*, addition of either antago-miR blocks the effect of WT1 on the EZH2 transcript level.

WT1(+KTS) Binds to a Recognition Motif in the EZH2 5′ UTR—Although it is known that the WT1(−KTS) isoforms regulate transcription of target genes in the nucleus, other investigators have noted that the WT1(+KTS) isoform can interact with RNA in the cytoplasm (16–22). This suggests that WT1(+KTS) may participate in the post-transcriptional regulation of targets such as *EZH2*. We screened the full-length *EZH2* transcript for the consensus WT1 recognition motif (23) using MatInspector software. This identified a classical motif, located 5 base pairs upstream of the ATG translational start codon in the *EZH2* 5′ UTR (Fig. 5*A*). To confirm binding to this site, we incubated *in vitro*-translated WT1(+KTS) protein with a radiolabeled oligomer corresponding to the sequence of the 5′ UTR containing the putative recognition motif. In Fig. 5*B*, a

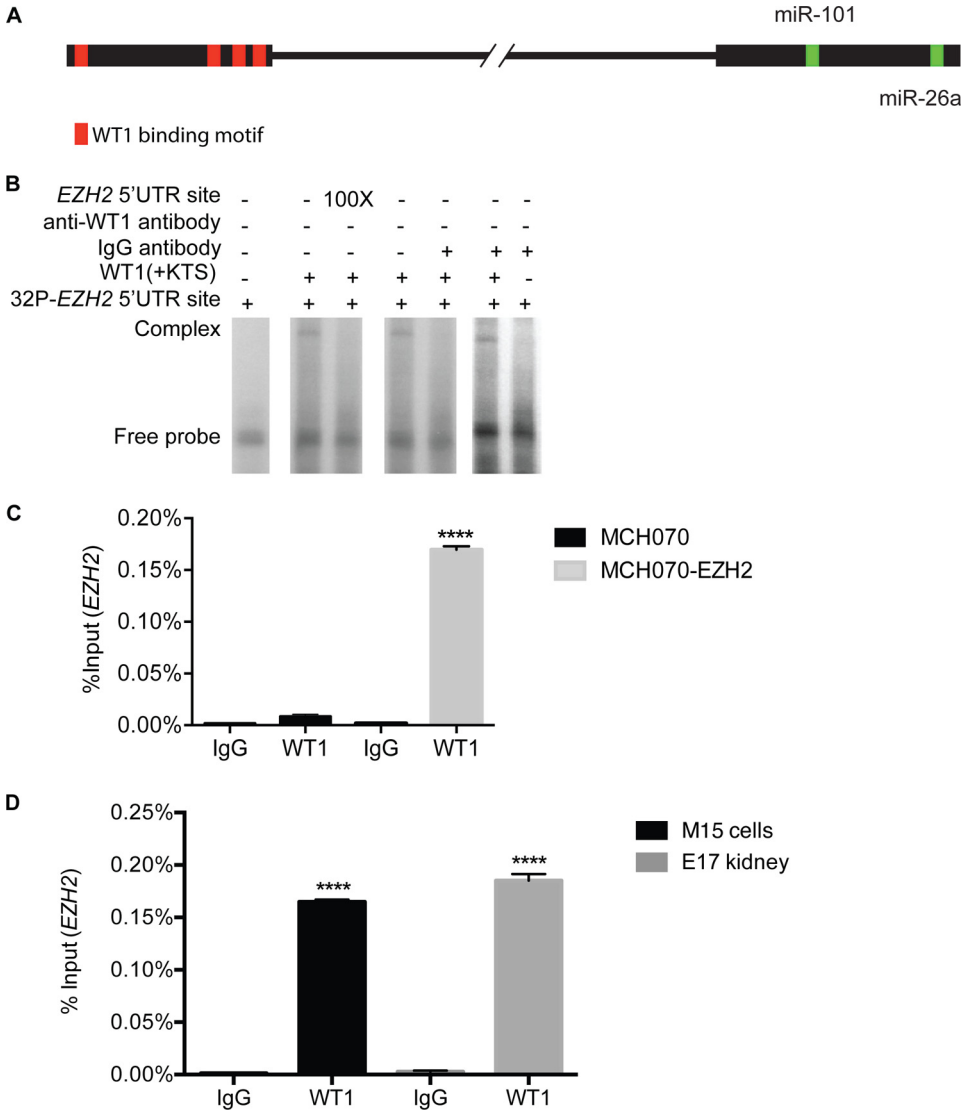

FIGURE 5. **WT1 binds the 5′ UTR of *EZH2*.** *A,* line drawing of the human *EZH2* gene sequence showing four putative WT1 recognition motifs (G*X*G*X*GG*X*G) in the 5′ UTR (*red boxes*), and the 8-nucleotide seed sequences for miR-26a (UACUUGAA) and miR-101 (GUACUGUA) in the 3′ UTR (*green boxes*). *B,* electromobility shift assay showing a high molecular weight complex containing the 5′ UTR site (18-mer) bound to *in vitro* translated WT1(+KTS) protein (*lanes 2* and *4*). This complex disappears in the presence of excess cold probe (*lane 3*) or specific antibody against WT1 (*lane 5*). The high molecular weight complex formed remains intact with IgG antibody (*lane 6*). *C,* mRNA associated with exogenous WT1 protein was immunoprecipitated from fibroblasts transfected with EZH2 plasmid (RIP) and *EZH2* RNA levels were quantified by qRT-PCR; WT1-associated *EZH2* mRNA levels are expressed as percent of total mRNA input. *D,* endogenous *EZH2* mRNA was immunoprecipitated with anti-WT1 antibody from a mouse mesonephric kidney cell line (M15 cells, *black bars*) and from mouse embryonic E17 kidneys (*gray bars*) and quantified by qRT-PCR. Unpaired *t* test, $p < 0.0001$ (****).

high molecular weight complex is evident; interaction between the WT1(+KTS) protein and oligomer can be competed out with excess cold probe or blocked with WT1-specific antibody (Fig. 5*B*). To confirm that WT1 binds to *EZH2* mRNA in whole cells, we extracted RNA from fibroblasts transfected with a CMV-EZH2 plasmid and incubated this with *in vitro*-translated WT1(+KTS). Following immunoprecipitation with anti-WT1 antibody, we quantified (qRT-PCR) *EZH2* mRNA associated with the WT1 protein. As seen in Fig. 5*C*, the *EZH2* transcript was detected in the anti-WT1 precipitate. To confirm that WT1 binds to the endogenous EZH2 transcript, we performed RNA-IP experiments followed by qRT/PCR. As seen in Fig. 5*D*, anti-WT1 antibody immunoprecipitates *EZH2* mRNA in embryonic day E17 mouse kidneys and in a mouse mesonephric kidney cell line (M15) (11).

Cytoplasmic WT1 Protein Is Detected in Progenitor Cells of Mouse Embryonic Kidney Cap Mesenchyme—If WT1(+KTS) interacts with cytoplasmic *EZH2* mRNA during normal kidney development, it should be detectable in the cytoplasm of progenitor cells in the cap mesenchyme of embryonic kidney. To confirm this, we performed immunofluorescent studies of embryonic day E17.5 mouse kidneys. WT1 protein was detected in both the nuclear and cytoplasmic compartments of cells in the cap mesenchyme (Fig. 6).

WT1 Directly Interacts with miR-26a- and miR-101-containing RISC—In Fig. 4, we noted that WT1(+KTS) and either miR26a or miR101 had a stronger inhibitory effect on fibroblast CMV-driven EZH2 expression than either molecule alone. We considered the possibility that this might involve direct interactions between WT1 at the *EZH2* 5′ UTR and the

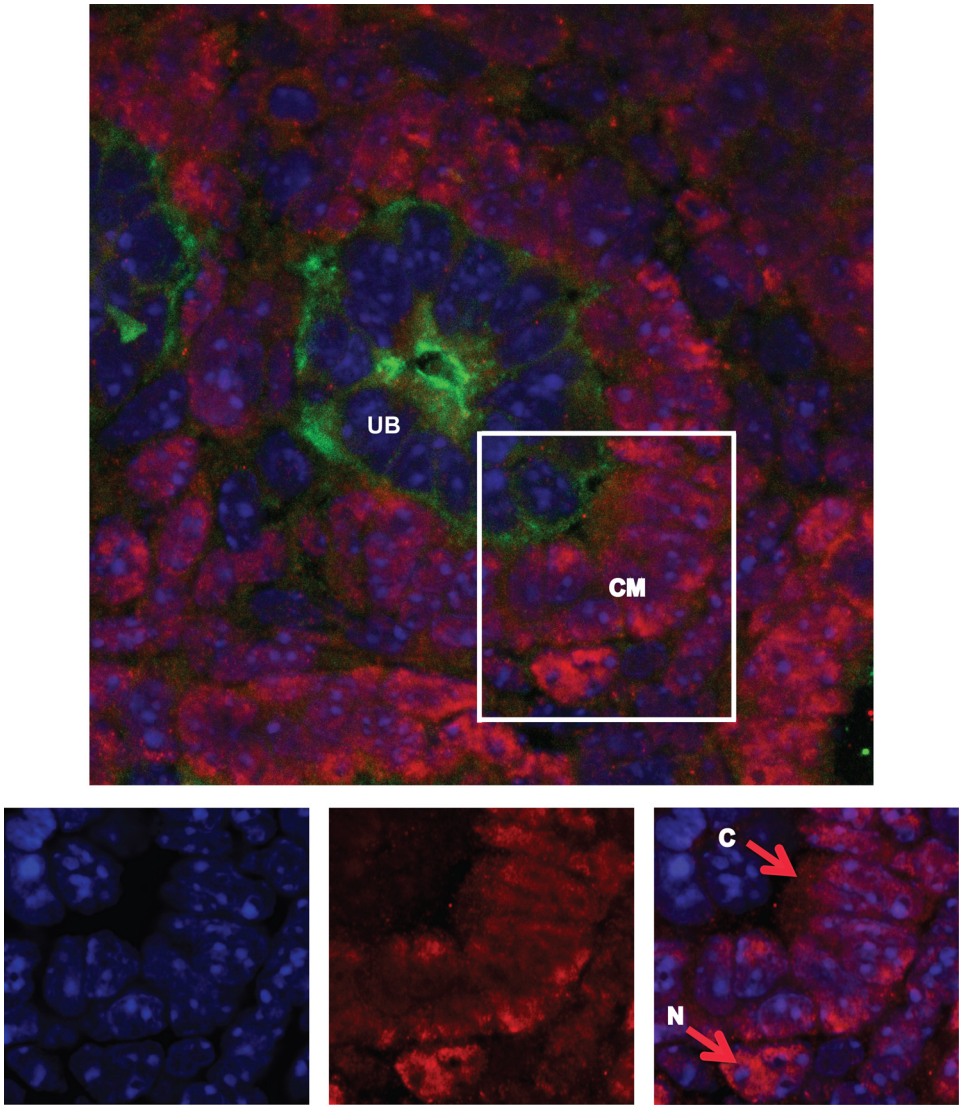

FIGURE 6. **Localization of WT1 within cap mesenchyme cells in embryonic mouse kidney.** Representative immunofluorescent image of embryonic mouse kidney at 17.5 dpc stained for WT1 (*red*), *D. biflorus* agglutinin (*DBA*) (*green*), and DAPI (*blue*). WT1 protein is seen in crescent of cells forming the cap mesenchyme (*CM*) around the ureteric bud (*UB*) branch tips stained with DBA (*top*). The magnified CM region (*lower panels*) shows nuclear DAPI staining (*bottom left*) and WT1 staining (*bottom middle*). The merged image shows both cytoplasmic (*C*) and nuclear (*N*) staining for WT1 (*bottom right*), emphasized by the *arrows*.

microRNA-containing RISC at the 3′ UTR. We lysed WT1(+KTS)-expressing amMSCs (or controls) and performed immunoprecipitation assays using antibodies specific for WT1, AGO2, DICER1, or IgG control (Fig. 7*A*). WT1 was precipitated with each member of the RISC. Conversely, when AGO2 or DICER1 were immunoprecipitated from the lysate, we were able to detect WT1 protein (Fig. 7*A*). To confirm that WT1 associates with the miRNA-containing RISC, we immunoprecipitated WT1 or AGO2 from cell lysates and screened for the presence of miR-26a, miR-101, and the EZH2 transcript by qRT-PCR. As seen in Fig. 7*B*, both miR-26a and miR-101 (but not miR-93, an unrelated miRNA lacking seed sequences in the transcript, not shown) were detectable in the WT1 and AGO2 precipitates. Similarly, we detected the *EZH2* transcript by qRT-PCR in both anti-WT1 and anti-AGO2 precipitates from mesenchymal stem cells transfected with WT1(+KTS). To confirm that the association of these molecules was not due to their common interaction with EZH2 mRNA, we treated the cell lysates with RNase A after immunoprecipitating with anti-DICER1, WT1, or AGO2 antibodies. Although full-length *EZH2* mRNA was no longer detectable by RT-PCR, we were still able to detect WT1 in association with each of its putative RISC partners (Fig. 7*C*).

Discussion

Mammalian kidneys arise from stem cells of the intermediate mesoderm. A subset of these cells begin to express WT1 and then acquire properties of nephron progenitors capable of responding to a canonical WNT signal; another subset of WT1(−) cells form the epithelial nephric duct and its caudal offshoot, the ureteric bud. As the ureteric bud begins to arborize, nearby nephron progenitors form a cap of tightly clustered cells around the tip of each ureteric bud branch these cells express WT1. As we show here, WT1 can be visualized both in

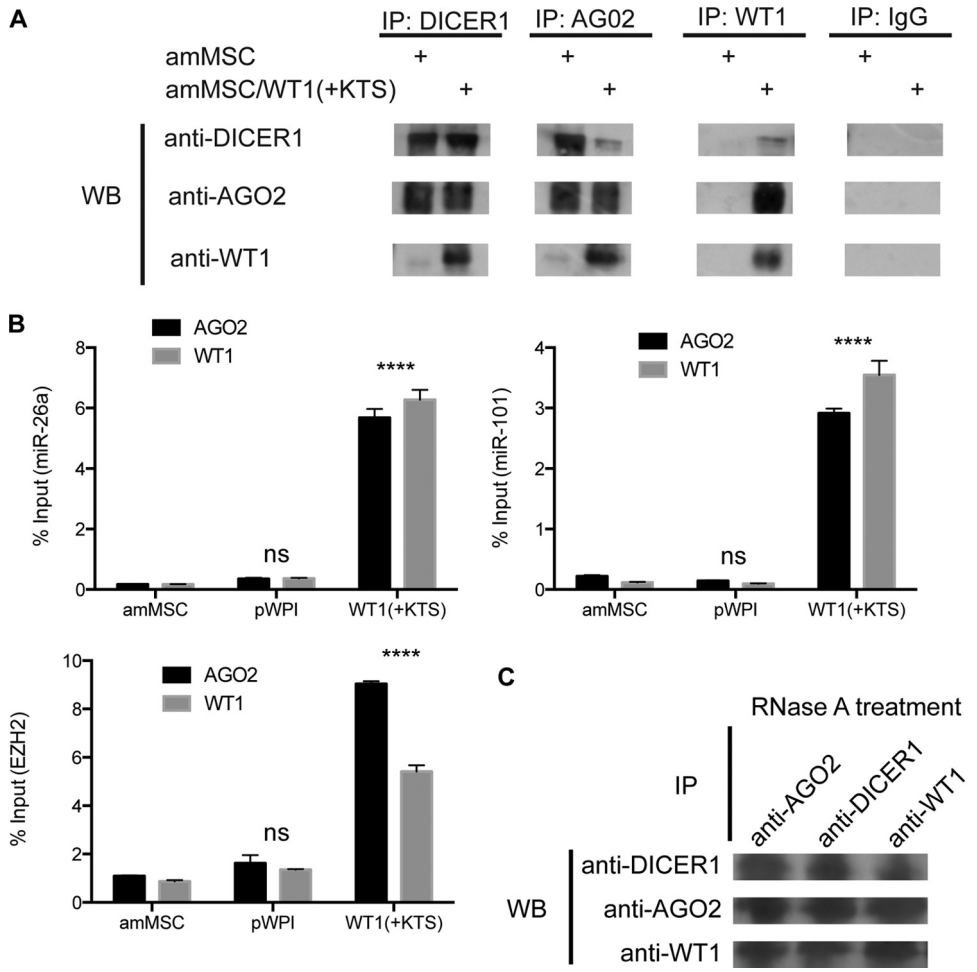

FIGURE 7. **Interactions of WT1, miRNAs, and RISC components.** *A*, representative Western blots (*WB*) probed with DICER, AGO2, or WT1 antibodies (*left*) of immunoprecipitates from amMSC *versus* amMSC/WT1(+KTS) using antibodies against DICER, AGO2, WT1, or control IgG (*top*). *B*, levels of *EZH2* mRNA, miR-26a, and miR-101 were quantified by RIP-qPCR in amMSC expressing WT1(+KTS) (*right bars*) *versus* amMSC with empty vector (*middle bars*) or uninfected parental amMSC (*left bars*). *Bar graphs* show levels of miR26a (*left upper*), miR101 (*right upper*), and EZH2 (*left lower*) as percent of total RNA input. Two-way analysis of variance with Tukey's multiple comparison tests were used to compare WT1(+KTS) amMSC with empty vector control amMSC; $p < 0.0001$ (****), not significant (*ns*). *C*, representative Western blot probed with DICER1, AGO2, or WT1 antibodies (*left*) of RNase A-treated immunoprecipitates (*top*) from amMSC/WT1(+KTS) cells.

the nucleus and cytoplasm of nephron progenitors in cap mesenchyme. In response to WNT9b released by the ureteric bud, nephron progenitors undergo a dramatic mesenchyme-to-epithelium transition and proceed to form all segments of the nephron.

In the nucleus of renal progenitors, we previously found that the WT1(−KTS) isoform suppresses transcription of a Polycomb histone methyltransferase, EZH2 (6). This event is likely to be essential if the differentiation cascade is to be released by inductive WNT signals from ureteric bud. Here we show that transcriptional inhibition of EZH2 is paralleled by translational inhibition in the cytoplasm by the WT1(+KTS) isoform. WT1 was co-immunoprecipitated with endogenous *EZH2* mRNA from embryonic kidney and a mesonephric cell line.

These findings support the observations of Hastie and coworkers (24), identifying a specific role for the WT1(+KTS) isoform in regulating RNA. We identified four classical WT1 recognition motifs in the 5′ untranslated end of the *EZH2* transcript and studied one of these in detail, showing that it binds WT1(+KTS) protein with high affinity. All four putative WT1 binding sites are positioned amid sequences recognizing proteins involved in mRNA translation. Thus WT1(+KTS) binding to the *EZH2* 5′ UTR is likely to disturb the translation initiation complex assembly. Exogenous EZH2 expression from a CMV-driven plasmid was suppressed *in vitro* by WT1(+KTS).

Translation of *EZH2* is also known to be controlled by specific microRNAs directed to seed sequences in its 3′ UTR. Two such miRNAs (miR-101 and miR-26a) suppress *EZH2* translation in other cellular settings (myoblasts and cancer cells) (12–14). Interestingly, we observed that both major WT1 isoforms induce expression (>2fold) of an overlapping array of 32 miRNAs in mesenchymal stem cells. These included miR-101 and miR-26a. About half of the 32 miRNAs have putative recognition motifs in the 5′ end of many other Polycomb protein transcripts. This suggests a concerted inhibitory mechanism by which WT1 isoforms broadly suppress expression of many Polycomb complex proteins that epigenetically silence differentiation cascade genes.

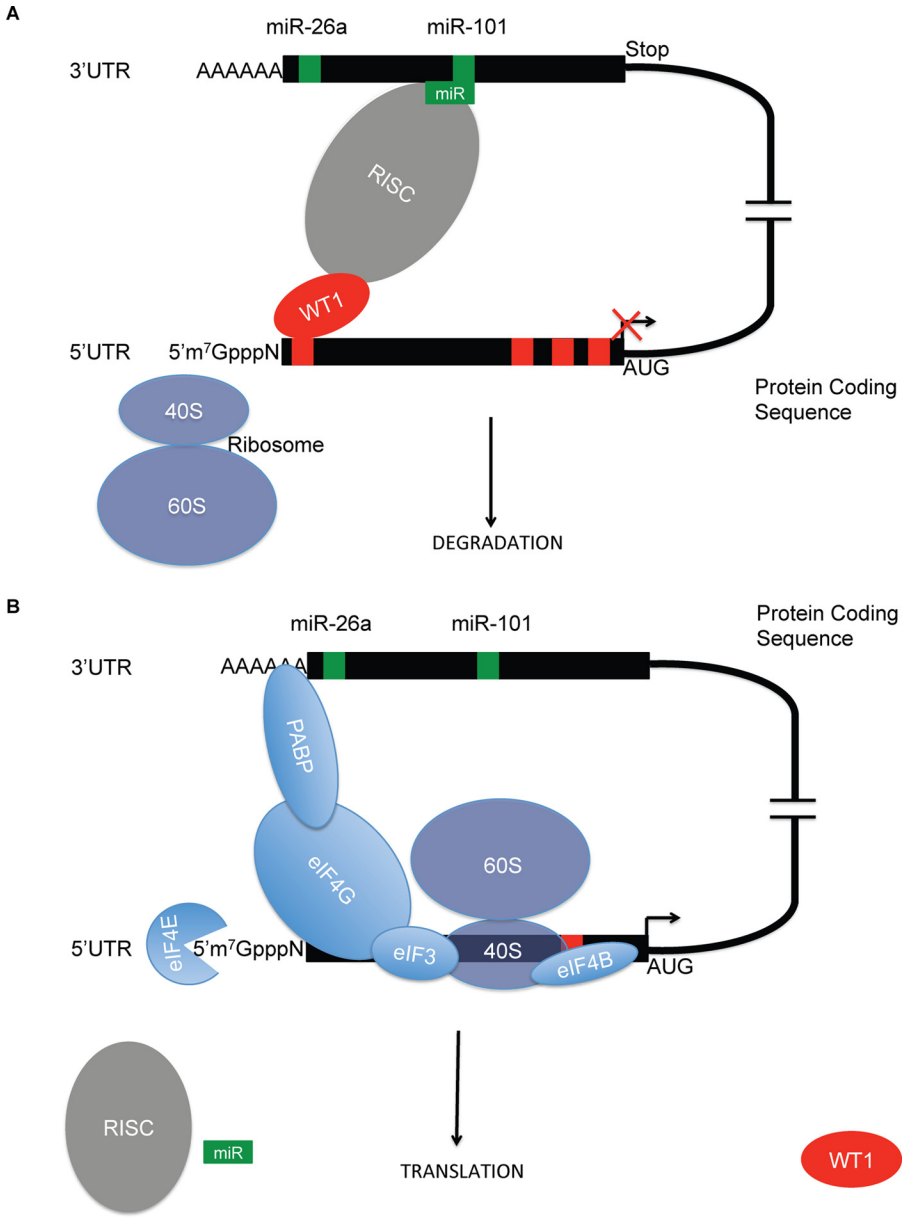

FIGURE 8. **Schematic model of WT1 post-transcriptional regulation of *EZH2*.** *A*, WT1(+KTS) (*red*) binds the 5′ UTR of the *EZH2* transcript and the miRNA(*green*)-containing RISC (*gray*) binds to the 3′ UTR seed sequence (*green*) to block access of the translation machinery. *B*, in the absence of WT1(+KTS) and miRNA-containing RISC, the 40S ribosome and translation complexes bind to the *EZH2* transcript 5′ UTR and promote protein translation.

In this study, we show that both WT1(+KTS) and exogenous miRNAs inhibit EZH2 in human fibroblasts. Remarkably, we found that addition of miRNA antagonists completely block the effects of WT1. Thus, cytoplasmic WT1(+KTS) bound to the 5′ UTR appears to cooperate with endogenous RISC-associated miRNAs bound at the 3′ UTR to disrupt translation.

miRNAs are a class of single-stranded non-coding RNA molecules containing 22 nucleotides (25, 26). Primary miRNAs (pri-miRNA) are transcribed in the nucleus by RNA polymerase II and processed by the DROSHA-DGCR8 complex into a stem-loop structure called the precursor miRNA (pre-miRNA) (27). Exportin-5 (XPO-5) transports the pre-miRNA out of the nucleus (28). In the cytoplasm, DICER1 processes the RNA molecule into the miRNA duplex (29). The strands are separated, the mature miRNA is recognized and bound by an AGO protein at the 3′ end and is integrated into the RNA-induced silencing complex (30). Through complementarity, the miRNA binds the 3′ UTR of the target messenger RNA (mRNA) (31). Perfect base pair match leads to degradation of the mRNA, whereas imperfect pairing will lead to sequestration of the mRNA and inhibition of translation (32). miRNAs play a crucial role in the regulation of mammalian development, their expression is tissue-specific, and tightly regulated spatial-temporally (33, 34).

Our immunoprecipitation studies indicate direct interaction between the WT1(+KTS) protein and DICER1/DROSHA (members of the RISC complex that mediates post-transcriptional mRNA decay and mRNA translation). Furthermore, immunoprecipitates containing WT1 and DICER/DROSHA also contained miR26a and miR101. Association between WT1

and the RISC was unaffected by prior experimental RNase degradation of the EZH2 transcript. These observations prompt a model, shown as a schematic in Fig. 8, in which WT1(+KTS) binds to motifs in the *EZH2* transcript 5′ UTR, which displace translation factors and inhibit translation; WT1 also interacts with RISC proteins targeted to the *EZH2* 3′ UTR by specific miRNAs and enhances their effects on transcript stability and protein translation.

In hereditary forms of Wilms tumor, biallelic loss of WT1 is thought to preclude the WNT response to WNT signals, resulting in a genetically unstable, developmentally arrested clone of progenitor cells; a second genetic "hit" then drives malignant transformation. Our observations demonstrate that the role of WT1 in de-repressing stem cell genes are, in part, dependent on specific microRNAs. We propose that this may explain why Wilms tumors may also arise from mutation of genes in miRNA processing.

Author Contributions—M. M. A. participated in experimental design, performed all *in vitro* experiments, analyzed the results, and participated in the preparation of the manuscript. L. L. C. performed the EMSA experiments. A. T. assisted with the qPCR validation. I. J. and L. H. assisted with the microRNA microarray analysis. E. T. provided WT1 immunofluorescent images in embryonic kidney. P. G. participated in experimental design, data analysis, and manuscript preparation. D. I. performed some of the experimentation, contributed to the design and analysis of other experiments, contributed to writing of the manuscript, and was co-supervisor for M. A. (first author, graduate student).

References

1. Rivera, M. N., and Haber, D. A. (2005) Wilms' tumour: connecting tumorigenesis and organ development in the kidney. *Nat. Rev. Cancer* **5,** 699–712
2. Call, K. M., Glaser, T., Ito, C. Y., Buckler, A. J., Pelletier, J., Haber, D. A., Rose, E. A., Kral, A., Yeger, H., and Lewis, W. H. (1990) Isolation and characterization of a zinc finger polypeptide gene at the human chromosome 11 Wilms' tumor locus. *Cell* **60,** 509–520
3. Fukuzawa, R., Heathcott, R. W., More, H. E., and Reeve, A. E. (2007) Sequential WT1 and CTNNB1 mutations and alterations of β-catenin localisation in intralobar nephrogenic rests and associated Wilms tumours: two case studies. *J. Clin. Pathol.* **60,** 1013–1016
4. Zirn, B., Samans, B., Wittmann, S., Pietsch, T., Leuschner, I., Graf, N., and Gessler, M. (2006) Target genes of the WNT/β-catenin pathway in Wilms tumors. *Genes Chromosomes Cancer* **45,** 565–574
5. Aiden, A. P., Rivera, M. N., Rheinbay, E., Ku, M., Coffman, E. J., Truong, T. T., Vargas, S. O., Lander, E. S., Haber, D. A., and Bernstein, B. E. (2010) Wilms tumor chromatin profiles highlight stem cell properties and a renal developmental network. *Cell Stem Cell* **6,** 591–602
6. Akpa, M. M., Iglesias, D. M., Chu, L. L., Cybulsky, M., Bravi, C., and Goodyer, P. R. (2015) Wilms tumor suppressor, WT1, suppresses epigenetic silencing of the β-catenin gene. *J. Biol. Chem.* **290,** 2279–2288
7. Ruteshouser, E. C., Robinson, S. M., and Huff, V. (2008) Wilms tumor genetics: mutations in WT1, WTX, and CTNNB1 account for only about one-third of tumors. *Genes Chromosomes Cancer* **47,** 461–470
8. Huff, V., Miwa, H., Haber, D. A., Call, K. M., Housman, D., Strong, L. C., and Saunders, G. F. (1991) Evidence for WT1 as a Wilms tumor (WT) gene: intragenic germinal deletion in bilateral WT. *Am. J. Hum. Genet.* **48,** 997–1003
9. Wu, M. K., Sabbaghian, N., Xu, B., Addidou-Kalucki, S., Bernard, C., Zou, D., Reeve, A. E., Eccles, M. R., Cole, C., Choong, C. S., Charles, A., Tan, T. Y., Iglesias, D. M., Goodyer, P. R., and Foulkes, W. D. (2013) Biallelic DICER1 mutations occur in Wilms tumours. *J. Pathol.* **230,** 154–164
10. Torrezan, G. T., Ferreira, E. N., Nakahata, A. M., Barros, B. D., Castro, M. T., Correa, B. R., Krepischi, A. C., Olivieri, E. H., Cunha, I. W., Tabori, U., Grundy, P. E., Costa, C. M., de Camargo, B., Galante, P. A., and Carraro, D. M. (2014) Recurrent somatic mutation in DROSHA induces microRNA profile changes in Wilms tumour. *Nat. Commun.* **5,** 4039
11. Larsson, S. H., Charlieu, J. P., Miyagawa, K., Engelkamp, D., Rassoulzadegan, M., Ross, A., Cuzin, F., van Heyningen, V., and Hastie, N. D. (1995) Subnuclear localization of WT1 in splicing or transcription factor domains is regulated by alternative splicing. *Cell* **81,** 391–401
12. Wong, C. F., and Tellam, R. L. (2008) MicroRNA-26a targets the histone methyltransferase Enhancer of Zeste homolog 2 during myogenesis. *J. Biol. Chem.* **283,** 9836–9843
13. Friedman, J. M., Jones, P. A., and Liang, G. (2009) The tumor suppressor microRNA-101 becomes an epigenetic player by targeting the polycomb group protein EZH2 in cancer. *Cell Cycle* **8,** 2313–2314
14. Friedman, J. M., Liang, G., Liu, C. C., Wolff, E. M., Tsai, Y. C., Ye, W., Zhou, X., and Jones, P. A. (2009) The putative tumor suppressor microRNA-101 modulates the cancer epigenome by repressing the polycomb group protein EZH2. *Cancer Res.* **69,** 2623–2629
15. Varambally, S., Cao, Q., Mani, R. S., Shankar, S., Wang, X., Ateeq, B., Laxman, B., Cao, X., Jing, X., Ramnarayanan, K., Brenner, J. C., Yu, J., Kim, J. H., Han, B., Tan, P., Kumar-Sinha, C., Lonigro, R. J., Palanisamy, N., Maher, C. A., and Chinnaiyan, A. M. (2008) Genomic loss of microRNA-101 leads to overexpression of histone methyltransferase EZH2 in cancer. *Science* **322,** 1695–1699
16. Charlieu, J. P., Larsson, S., Miyagawa, K., van Heyningen, V., and Hastie, N. D. (1995) Does the Wilms' tumour suppressor gene, WT1, play roles in both splicing and transcription? *J. Cell Sci. Suppl.* **19,** 95–99
17. Niksic, M., Slight, J., Sanford, J. R., Caceres, J. F., and Hastie, N. D. (2004) The Wilms' tumour protein (WT1) shuttles between nucleus and cytoplasm and is present in functional polysomes. *Hum. Mol. Genet.* **13,** 463–471
18. Caricasole, A., Duarte, A., Larsson, S. H., Hastie, N. D., Little, M., Holmes, G., Todorov, I., and Ward, A. (1996) RNA binding by the Wilms tumor suppressor zinc finger proteins. *Proc. Natl. Acad. Sci. U.S.A.* **93,** 7562–7566
19. Zhai, G., Iskandar, M., Barilla, K., and Romaniuk, P. J. (2001) Characterization of RNA aptamer binding by the Wilms' tumor suppressor protein WT1. *Biochemistry* **40,** 2032–2040
20. Morrison, A. A., Viney, R. L., Saleem, M. A., and Ladomery, M. R. (2008) New insights into the function of the Wilms tumor suppressor gene WT1 in podocytes. *Am. J. Physiol. Renal Physiol.* **295,** F12–17
21. Morrison, A. A., Viney, R. L., and Ladomery, M. R. (2008) The post-transcriptional roles of WT1, a multifunctional zinc-finger protein. *Biochim. Biophys. Acta* **1785,** 55–62
22. Morrison, A. A., Venables, J. P., Dellaire, G., and Ladomery, M. R. (2006) The Wilms tumour suppressor protein WT1 (+KTS isoform) binds α-actinin 1 mRNA via its zinc-finger domain. *Biochem. Cell Biol.* **84,** 789–798
23. Nakagama, H., Heinrich, G., Pelletier, J., and Housman, D. E. (1995) Sequence and structural requirements for high-affinity DNA binding by the WT1 gene product. *Mol. Cell. Biol.* **15,** 1489–1498
24. Davies, R., Moore, A., Schedl, A., Bratt, E., Miyahawa, K., Ladomery, M., Miles, C., Menke, A., van Heyningen, V., and Hastie, N. (1999) Multiple roles for the Wilms' tumor suppressor, WT1. *Cancer Res.* **59,** 1747–1750
25. Krol, J., and Krzyzosiak, W. J. (2004) Structural aspects of microRNA biogenesis. *IUBMB Life* **56,** 95–100
26. Winter, J., Jung, S., Keller, S., Gregory, R. I., and Diederichs, S. (2009) Many roads to maturity: microRNA biogenesis pathways and their regulation. *Nat. Cell Biol.* **11,** 228–234
27. Lee, Y., Ahn, C., Han, J., Choi, H., Kim, J., Yim, J., Lee, J., Provost, P., Rådmark, O., Kim, S., and Kim, V. N. (2003) The nuclear RNase III Drosha initiates microRNA processing. *Nature* **425,** 415–419
28. Lee, Y., Kim, M., Han, J., Yeom, K. H., Lee, S., Baek, S. H., and Kim, V. N. (2004) MicroRNA genes are transcribed by RNA polymerase II. *EMBO J.* **23,** 4051–4060
29. Kim, V. N., Han, J., and Siomi, M. C. (2009) Biogenesis of small RNAs in

animals. *Nat. Rev. Mol. Cell Biol.* **10,** 126–139
30. Elbashir, S. M., Lendeckel, W., and Tuschl, T. (2001) RNA interference is mediated by 21- and 22-nucleotide RNAs. *Genes Dev.* **15,** 188–200
31. Gagnon, K. T., and Corey, D. R. (2012) Argonaute and the nuclear RNAs: new pathways for RNA-mediated control of gene expression. *Nucleic Acid Ther.* **22,** 3–16
32. Nelson, P., Kiriakidou, M., Sharma, A., Maniataki, E., and Mourelatos, Z. (2003) The microRNA world: small is mighty. *Trends Biochem. Sci.* **28,** 534–540
33. Zhao, Y., and Srivastava, D. (2007) A developmental view of microRNA function. *Trends Biochem. Sci.* **32,** 189–197
34. O'Rourke, J. R., Swanson, M. S., and Harfe, B. D. (2006) MicroRNAs in mammalian development and tumorigenesis. *Birth Defects Res. C Embryo Today* **78,** 172–179
35. Cone, T. E., Jr. (1970) Sir William writes about massive abdominal tumors in children. *Pediatrics* **46,** 587